

A Molecular Dynamics Simulation of the Toluene-Water Interface in the Presence of an External Magnetic Field

K. Khajeh^{†1}, H. Aminfar¹ and M. Mohammadpourfard²

¹Mechanical Engineering Department, University of Tabriz, Tabriz, East Azerbaijan, 5166616471, Iran

²Faculty of Chemical and Petroleum Engineering, University of Tabriz, Tabriz, Iran

[†]Corresponding Author Email: k.khajeh.2005@tabrizu.ac.ir

(Received January 25, 2020; accepted May 13, 2020)

ABSTRACT

Among the current techniques in the stabilizing the emulsion, the magnetic treatment is attracting more attention during past years. In this work, a molecular dynamics simulation was performed to investigate the effect of an external magnetic field on the toluene-water interface. An extended version of Nanoscale Molecular Dynamics (NAMD) source code including the magnetic field feature was used to do all MD calculations. The radial distribution function (RDF), the integration RDF, and the non-bonded energy of three pairs atoms, beside the interfacial tension (IFT) values in the presence of different magnetic field intensities have been calculated and reported in this paper. The changes in the potential of the interaction has been proved by analyzing the RDF and integration RDF plots. The obtained results showed that the increase of IFT is only appeared within a specific range of magnetic field intensities. Moreover, the IFT decreases when the magnetic field intensity is increased. The simulation results provide an elementary understanding of the applying magnetic treatment as a technique in the preparing of emulsion system.

Keywords: Magnetic field; Interfacial tension; Emulsion; Molecular dynamics simulation; Interaction.

NOMENCLATURE

A	interfacial area	r	position of atom
a	acceleration	t	time
B	magnetic field intensity	T	temperature
F	force	U	force field
e_z	unit vector	V	velocity
L	box length	x, y, z	coordination
M	mass		
N	number of atoms in the box simulation		
P	pressure	γ	interfacial tension
q	charge of atom	Ω	larmor frequency

1. INTRODUCTION

A system which consist two immiscible liquids is generally called emulsion. The dispersed droplets (internal phase) are stably suspended in the continuous (external) phase. During the past years, a great effort has been made to characterize the specifications of three types of emulsions; water-in-oil (W/O) emulsion, oil-in-water (O/W) emulsion, and multiple emulsion (Langevin *et al.* 2004; Souleyman 2015; Kilpatrick 2012; Wong *et al.* 2015). It is a great interest of researchers

introducing the interfacial active molecules for the oil-water interface to stabilize the emulsion in different industries such as pipeline transporting (Kumar and Mahto 2017), oil based drilling fluid (Huang *et al.* 2018), emulsion fuel in a diesel engine (Souleyman 2015), food emulsions (Andresen, 2007) and etc., (Langevin *et al.* 2004; Ruiz-Morales and Mullins 2015). Using emulsifying agent forms a stable emulsion based on the different mechanisms; delay in coalescence and creaming due to forming the film coating around each droplet of dispersed phase, retarding the

movement of droplets due to increment in viscosity of continuous phase, and etc., ...

The preparation of emulsions requires energy to disperse the organic phase in water. An emulsifier reduces the surface tension at the oil-water interface, and protects the newly formed droplet interfaces from immediate coalescence. In the absence of any emulsifying agent, emulsion system is unlikely, and through time, the phase separation will occur. The high interfacial tension (IFT) between two phases makes this phase splitting. In fact, the high IFT value between two immiscible liquids induce an attractive force between the molecules of each phase. Then, the same molecule types are merged quickly, and finally, two individual phases are appeared. Currently, to stabilize the emulsion system, adding the surface active agent (or emulsifier) as the third phase is widely used (Sheng, 2013). Andresen *et al.* (2007) investigated the characteristics of water-in-toluene emulsions stabilized solely by hydrophobized microfibrillated cellulose. They reported the emulsions are considerably stable against coalescence and drop size decreases in their tests. Maphosa *et al.* (2018) showed the application of polysaccharides in emulsion systems caused an improvement in stabilization properties.

In recent decades, molecular dynamics (MD) simulation was carried out to improve the understanding of the interfacial system (Allen, 2004; Israelachvili, 2011).

During the past years, magnetic treatment is getting more attention among the current techniques to affect thermodynamics behavior of the system. Magnetic treatment is currently an ongoing approach in the oil field to change viscosity (Moosavi and Gholizadeh 2014). Moosavi and Gholizadeh (2014) by using DL-POLY package studied the effect of an external constant magnetic field at ambient temperature and pressure on the thermo-physical properties of organic solvents and water. They reported that the hydrogen bond is strengthened in the presence of magnetic field, and the density is increased. Also, they showed that diffusivity and mobility of the solvent are decreased under the effect of the magnetic field. They related this to the significant changes in the molecular structure under the influence of the magnetic field. Chen *et al.* (2018) by employing the MD simulation by using LAMMPS (Large-scale Atomic/Molecular Massively Parallel Simulator) software and OPLS-AA(Optimized Parameters for Liquid Simulations All- Atom) force field reported the effect of the magnetic field on the waxy crude oil. This light oil included different types of alkanes and aromatics. Based on their results, the high and low intensities of the magnetic field exhibit an adverse effect on the density, diffusion coefficient, and viscosity of the mixture. Also, they reported the more significant influence of magnetic field on the morphology compared to distances between molecules. Recently, Saeedi Dehaghani and Badizad (2018) investigated the displacing effect of the CTAB nano-emulsion in oil through porous space of a silicon packed core in the presence and

absence of pre-treatment magnetized condition. They obtained slightly higher value for interfacial tension of nano-emulsion. They reported that exposing the nano-emulsion to the magnetic field leads to the lower mobility ratio during the flooding process. For the first time, Peng *et al.* (2012) examined the breaking effect of magnetized demulsifier on the water-in-diluted bitumen emulsions. They introduced this surface-active polymer grafted on magnetic nanoparticles as a high-efficiency demulsifier. They encouraged others to use this new technique, and take advantage of rapid kinetics in physical separation water from heavy oil.

Tung *et al.* (2001) tested experimentally the paraffin crystallization of crude oil in the presence of a magnetic field. They observed that the sample containing more polar particles such as resin and asphaltene is more affected. They also reported about 20-25% reduction in a wax deposition for all considered test samples. Finally, they introduced magnetic treatment as a promising technique to improve the liquidity of paraffin crude oil. Guo *et al.* (2011), by employing MD simulation, studied the diffusion of three applicable cations in seawater; sodium ion, magnesium ion, and calcium ion. They found out the magnetic field is an effective separation process for brine from seawater due to the increase in diffusion coefficients of cations.

From this short review, it is understood that only a few works have done to demonstrate the effect of an external magnetic field on the thermo-physical behavior of the emulsion system. This study is a primary effort to illustrate the characteristics and mechanism of the toluene-water interface in the presence of an external magnetic field.

It is noticeable that most of the work in this area have been done in the field strength of up to 10 T (Chen *et al.* 2018; Chang and Weng, 2006; Han 2013) (These are molecular simulation study) and Iwasaka and Ueno (1998) (this is an experimental work). These studies encouraged us to investigate our interfacial system in this range of the magnetic field intensity. On the other hand, the molecular simulation technique gives insight about problems which are difficult to test under laboratory conditions or investigations are expensive. That's why we decided to study the interfacial system in a wide range of magnetic field intensities.

This work aimed to identify the result as; the Radial Distribution Function (RDF) plot, the integration RDF plot, density distribution along the box length, IFT values, and the non-bonded energy values for different pairs of atoms.

At the next section, the procedure of adding the magnetic field as the new feature into an MD simulation package is introduced. Then, the MD simulation setup, some considerations, and details are expressed. After that, the verification of the simulation method is described. At the end, all obtained results are presented and discussed, and the main conclusions of present work are reported.

2. COMPUTATIONAL METHODS

In this work, all molecular structures were generated by using Avogadro software (version 1.2.0) (Hanwell *et al.* 2012). The boxes were built by using Packmol (Martinez *et al.* 2009). The initial configurations for molecular dynamics simulations by optimization in packing is obtained by using Packmol. The free software VMD (Visual Molecular Dynamics) was used to visualize the obtained data in the graphical page (Humphrey 1996). Both Density Profile Tool (Giorgino 2014) and Diffusion coefficient tool (Giorgino 2019) were added to VMD to analyze data in detail. Parallel free MD simulator package, NAMD (NANoscale Molecular Dynamics) (Phillips *et al.* 2005) and CHARMM 37 (Chemistry at HARvard Molecular Mechanics) (Brooks *et al.* 2009) force field were performed to do all calculations. The force field is used extensively in the simulations of hydrocarbons at similar conditions.

2.1 External magnetic field

Since the NAMD has not been designed for considering the effects of the magnetic field, the first part of this paper is devoted to introducing the implementation method of the magnetic force inside the velocity verlet (VV) algorithm. When the moving charged particle q with velocity V , is exposed to an external constant magnetic field with intensity vector B , the motion of the charged particle is affected by Lorentz force as below;

$$F=q(\mathbf{V}\times\mathbf{B}) \quad (1)$$

This external force changes the total acceleration in an MD algorithm (Spreiter and Walter 1999). By introducing the magnetic field based on the Lorentz force in the z -direction, the velocity verlet algorithm is modified. The position and velocity at the next time step ($r(t+\Delta t)$, $V(t+\Delta t)$) from the current one ($r(t)$, $V(t)$) are obtained by Eqs. (2 and 3);

$$r(t+\Delta t) = r(t) + [\Delta t.V(t)] + \{(\Delta t^2/2).[a(t)-\Omega e_z \times V(t)]\} \quad (2)$$

$$V(t+\Delta t) = V(t) + (\Delta t/2).\{[a(t)-\Omega e_z \times V(t)] + a(t+\Delta t)-\Omega e_z \times V(t+\Delta t)\} \quad (3)$$

r is coordinate of atoms, a is the acceleration of atoms, Δt is time step. The Larmor frequency is defined as; $\Omega = \frac{qB}{m}$ [A particle of specific charge

$\frac{q}{m}$ performs Larmor oscillations of frequency

$$\Omega = \frac{qB}{m} \text{ when influenced by a magnetic field } B,$$

and $e_z = (0,0,1)$ which is the unit vector in z -direction. The time step should be small enough to follow the trajectory of each particle in the simulation. The modified Velocity Verlet algorithm inside the NAMD source code is presented in Fig.1 (Numbers *et al.*1998; Khajeh *et al.* 2020).

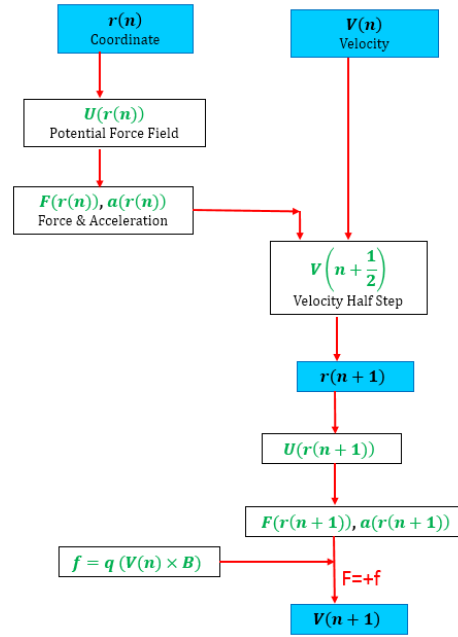


Fig. 1. Performing the magnetic field into the Velocity Verlet algorithm in NAMD. q is the charge, B is the magnetic intensity, r is coordinate of atoms, a is the acceleration of atoms, V is the velocity of atoms, U is force field, n is time step, F is the force.

2.2 MD Simulation Setup

Here, the details of the MD simulation is given. A simulation box contains 7500 SPC/E (single point charge/extended) water molecules, and 1000 toluene molecules. In this work, the SPC/E model has been performed, as it can reproduce the surface tension of water as well as other structural properties of liquid water (Kunieda *et al.* 2010; Alejandre *et al.* 1995).

All simulations were done at ambient temperature and pressure, 300 K and 1.01 bar, respectively. The periodic boundary condition was employed in 3 dimensions. The non-bonded interactions and long-range coulombic interactions were calculated by Lennard-Jones potential and PME (Particle Mesh Ewald) summation (Kunieda *et al.* 2010). The cut-off radius for all cases was considered 12 Å. Langevin dynamics thermostat was used as a coupling temperature algorithm (Kunieda *et al.* 2010). The time interval 1 fs was set to all simulations. The effect of an external magnetic field in z -direction have considered, and the IFT, RDF, density profile, non-bonded energy values are reported.

2.2 MD Validation

In this part, the verification of the simulation setup in several steps are presented. The first step in this work is to model and verify the result of employing the magnetic field on the water box. This procedure has done for a cubic box containing 901 SPC/E water molecules at environmental temperature and pressure. The self-diffusion coefficient was

calculated and compared to available data reported in [Chen *et al.* \(2018\)](#) and [Chang and Weng \(2006\)](#). Table. 1 shows a good agreement between data in present work and reported results. The small difference between these results is due to using different force field and different water model in these simulations.

Table 1 Comparison results of self-diffusion coefficient of the water in the presence and absence of magnetic field

	B=0 [T]	B=7 [T]	Changing ratio (%)	details
Present work	2.46	2.25	8.71	901 SPC/E model water molecules, CHARMM, NAMD
Chen <i>et al.</i> (2018)	2.62	2.38	8.92	1728 SPC/E model water molecules, CHARMM, LAMMPS
Chang and Weng (2006)	2.14	2.01	6.20	4096 F3C model water molecules, developed code

Since we have used the toluene as the oil phase in our work, the toluene density (1000 toluene molecules in the simple cubic box) was obtained and compared to experimental and simulation results reported in literature ([Mikami *et al.* 2013](#)). Table 2 shows a very close agreement with experiment ([Lemmon *et al.* 2002](#)) and another MD simulation ([Kunieda *et al.* 2010](#)).

Table 2 Density of toluene [kg/m³] at 300 K and 1.01 bar

Experimental data	862.38 (Lemmon <i>et al.</i> 2002)
Simulation results	867.45 (Kunieda <i>et al.</i> 2010)
Present work	865.48

IFT is the most critical parameters in introducing the interfacial system. In our work, the isobaric-isothermal-iso interfacial area (NPA_nT) ensemble was used to simulate the interface system ([Mikami *et al.* 2013](#)). The box length in two directions were kept fixed at 5.6 nm during the calculation to reproduce the iso-interfacial area condition on the system. In all simulations, both the temperature and the pressure were kept constant by Langevin dynamics thermostat and barostat ([Kunieda *et al.* 2010](#)). Continuing the calculation for 5 ns is close enough to equilibrium, and as seen in Fig. 2, the rolling average of IFT indicates the simulation was done at enough time. The time step was 1 fs, and the atomic coordinates were updated every 1.0 ps. Due to periodic boundary conditions performed in our

MD simulations, all systems represent two identical toluene-water interfaces. IFT for two identical interfaces perpendicular to the z-axis, were calculated as following ([Kunieda *et al.* 2010](#));

$$\gamma = (12)(P_z - ((P_x + P_y)/2)).L_z \quad (4)$$

P_x , P_y and P_z are the diagonal components of the pressure tensor, and the L_z is the box length in z-direction. In the case of the toluene-water system, the IFT was calculated by Eq.4. We obtained the IFT of toluene-water to confirm that our MD simulation can successfully predict the interface properties of water and hydrocarbons. The IFT value was 37.44 mN/m, which is in good agreement with experimental and other MD data ([Kunieda *et al.* 2010](#)). Table 3 reports the IFT value in this work compared to calculated experimental and MD simulations in literature. Also, Fig. 2 exhibits the rolling average of IFT to emphasis that the equilibrium is fully achieved, and all data were gathered and analyzed in the equilibrated phase. The density profile along the box length was obtained by taking the time average over the last 2 ns of the 5 ns calculations.

Table 3 Interfacial tension of toluene-water [mN/m] at 300 K and 1.01 bar

Experimental data	36.40, 36.10, 36.00 (Donahue 1952)(Moran <i>et al.</i> 1999)
Simulation results	37.69 (Kunieda <i>et al.</i> 2010)
Present work	37.44

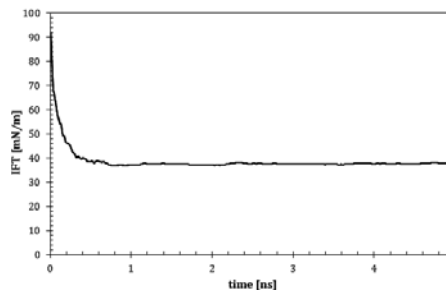


Fig. 2. Rolling average of IFT for the toluene-water interface system at ambient temperature and pressure.

3. RESULTS AND DISCUSSION

In this work, the interface between toluene and water is studied in the presence of the magnetic field (B=0, 2, 4, 6 [T]) as an external constant force. In following, the effect of the magnetic field on the RDF, integration RDF, non-Bonded energy and IFT values are reported. The RDF is usually used to investigate the structure of the molecules.

The RDF is defined as the number of atoms in a shell of thickness for an arbitrary atom at a distance from the origin atom. The RDF is calculated as Eq. 5 ([Moosavi and Gholizadeh 2014](#));

$$g(r) = \{ \langle N(r, \Delta r) \rangle \} / \{ (1/2)N \rho V(r, \Delta r) \} \quad (5)$$

where angular brackets indicate a temporal average;

$N(r,\Delta r)$ is the number of atoms within a spherical shell of radius between r and $r+\Delta r$; N the total number of atoms in the system; ρ the number density, and $V(r,\Delta r)$ is the volume of the shell.

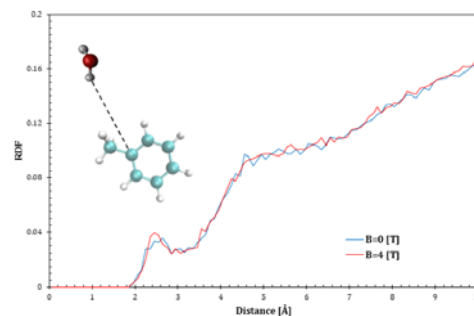
Figure 3 shows the RDF between the central atom of the toluene molecule, and the oxygen and the hydrogen of the water. This figure presents the RDF ($O_{\text{water-C}}$) and RDF ($H_{\text{water-C}}$), i.e., the distribution of the water atoms in any direction from the center of the toluene molecule. This plot has been reported for the magnetic field intensity of $B=0$, and $B=4$ [T] to discuss about the intermolecular interaction level at toluene-water interface. As seen in this figure the RDF plot in the case of absence of magnetic field is similar to the results of [Kunieda *et al.* \(2010\)](#). The highest values in the case $H_{\text{water-C}}$ (i.e., the Fig.3-a) around the 2.5 Å is increased. From the Fig. 3-b ($O_{\text{water-C}}$), it is illustrated that the highest values around the 3.5 and 5 Å are increased in the presence of the magnetic field.

This slight increase in the highest value of RDF indicates that the potential for interaction between two phases is positively influenced by applying an external magnetic field. Besides, this slight increase is in good agreement with RDF plot for pure water atoms in the presence of magnetic field ([Chang and Weng 2006](#)). Besides, this small increase in the height of the peak indicates that more toluene molecules are located between the water shells. It can be understood that the magnetic field forces more carbon atom between the water shells. The magnetic field by reforming the structure of the interface leads to increase the connectivity of two phases, and the stability of the network of $O_{\text{water-C}}$ and $H_{\text{water-C}}$ improves.

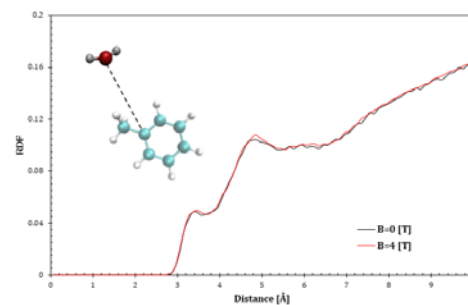
The number of surrounding atoms in vicinity of atom interest is called the coordination number which can be introduced here by integration RDF. ([Carrillo Beber *et al.* 2015](#)). We calculated the area under the RDF plot and reported the integration RDF in Fig. 4. This plot shows that the potential for interaction is changed in the presence of different magnetic field intensities. The number of atom pairs presented at a specific distance decreases when the magnetic field intensity range is from 0 to 2 [T], and is increased under the effect of much intense magnetic field. Comparing the integral RDF for different magnetic field intensities ($B=0, 2, 4, 6$ [T]) are presented in Fig. 4. The atom pairs H-C and O-C in the presence and absence of magnetic field show the same trend under the effect of different magnetic field intensities.

[Kunieda *et al.* \(2010\)](#) reported that the interfacial tension between water and aromatics are lower than other hydrocarbons. They illustrated that the RDF plot between water atoms and toluene have two peaks. They showed that the water molecule is perpendicular to the toluene ring, and the hydrogen atom of the water molecule orients toward the center of the toluene ring. They attributed this interaction to the weak hydrogen bonding between the aromatic rings and the water protons. Finally, they introduced this mechanism as a factor in reducing the interfacial tension. This weak

hydrogen bonding illustrates an inherently attractive effect. From a deeper perspective, the high potential interaction between two types of molecules (present at the interface) causes a reduction in IFT value.



a)



b)

Fig. 3. The RDF plot at 300K and 1 bar between; (a): the center of the toluene molecule and hydrogen atom in the water molecule, and (b): the center of the toluene molecule and oxygen atom in the water molecule (red line, $B=4$ [T], and blue line $B=0$ [T]).

The results in Fig. 4 represent the information on the distance between atom pairs ($O_{\text{water-C}}$ and $H_{\text{water-C}}$) which are of interest for the possible interaction between the atoms in these two atom pairs. It can be obtained from this figure that the amount of IFT for the case of $B=6$ [T], and $B=2$ [T] are less and more than $B=0$, respectively.

In order to investigate the impact of a magnetic field on the toluene-water interface, the IFT values have been calculated and reported in Table 4 based on the Eq. 4. As expected, the IFT value increases in the applied magnetic field range of 0-2 [T]. However, it decreases under the effect of applying the stronger magnetic fields (higher than 2 [T]). It means that employing the magnetic field (stronger than 2[T]) exhibits the “decreasing effect on IFT” same as increasing temperature ([Jennings 1967; 1971](#)). Although there is small difference between the results obtained with and without the magnetic field, these results are consistent with other reported data in this area ([Chang and Weng 2006; Chen *et al.* 2018](#)). It is also worth noting that all calculations in this work have been repeated three times, and the average has been reported.

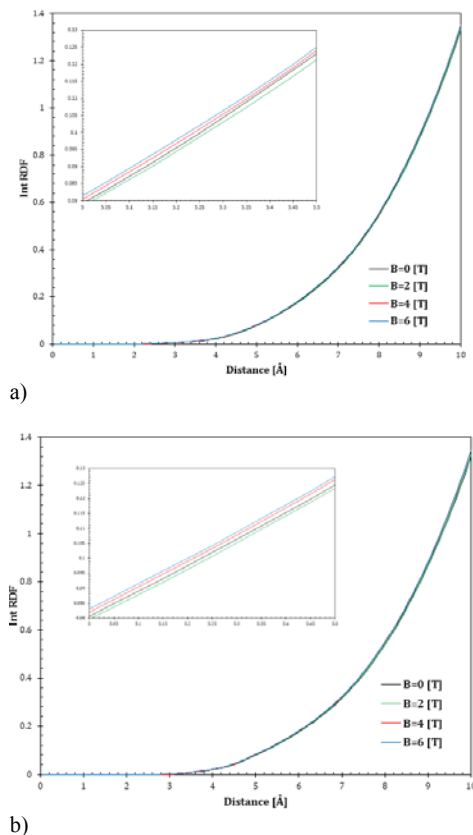


Fig. 4. The integral of the RDF for pairs of atom C in the toluene molecule, and water atoms; (a) H-C, (b) O-C, in the presence of different intensities of the magnetic field.

Table 4 IFT values for the toluene-water interface at 300 K and 1 bar in the presence of and absence of magnetic field

Magnetic field Intensity [Tesla]	B=0	B=1	B=4	B=6
Interfacial tension [mN/m]	37.44	38.40	35.45	34.32
Percentage of change in IFT value [%]	-	+2.5	-5.3	-8.3

The IFT is described as the amount of work which should be expended to mix the two immiscible liquids or to increase the interfacial area between the two adjacent phases. It is difficult to form a stable emulsion of water and toluene while the interfacial tension is high. Currently, adding emulsifiers is known as a useful technique to decrease IFT. It has been reported that the IFT value achieves much reduction by increasing the amount of concentration of surfactant and other chemical additives (Alomair *et al.* 2015; Kumar and Mahto 2017). Emulsifiers prevent from the aggregation and coherence of dispersed phase droplets by reducing the interfacial tension. In other words, adding emulsifier to the system, by reducing the IFT, contributes to the stability of the emulsion system. It is understood from the calculated IFT

values in Table 4 that in the presence enough strong magnetic field, smaller size droplets of toluene or water are formed (depends upon to this fact that we are considering the O-W or W-O emulsion). Here, reduction in IFT value illustrates the emulsifying behavior of the strong magnetic field for the cases; B=4 and 6 [T] at 300K and 1.01 bar. In the absence of the magnetic field, the high interfacial energy between toluene and water forms a minimum surface area between two liquids. When the strong magnetic field is applied, a more stable emulsion (between toluene and water) is obtained.

A typical snapshot of a unit cell for the MD calculation of the interface system under 300 K and 1.01 bar is shown in Fig. 5. The interface with a width (10%–90% width (Pohorille 1993) approximately 6 Å is observed.

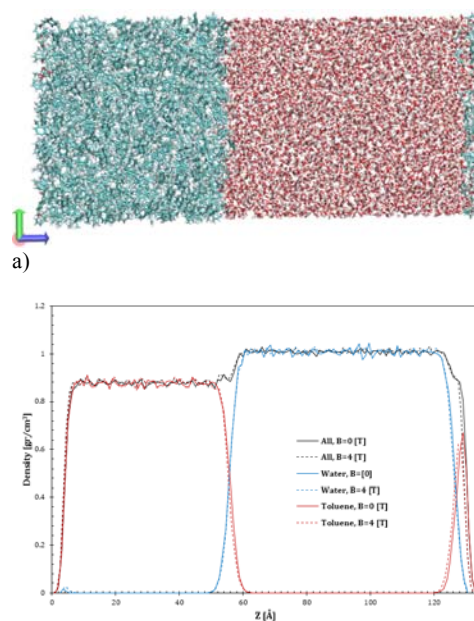


Fig. 5. (a) snapshot of the toluene-water interface system at 300 K and 1 bar in the presence of magnetic field (B=4 T) taken after 5.0 ns of NPnAT simulation (red, oxygen atom; blue, carbon atom; grey, Hydrogen). (b) The density profiles of the total interfacial system, toluene, and water; along the z-axis averaged over 3.0-5.0 ns at 300 K and 1 bar (red, toluene; blue, water; black, all).

An MD simulation includes two types of interactions; van der Waals interactions and Coulomb interactions. The former one is a dispersive interaction which is caused by temporary fluctuations of the charge distribution in the atoms or molecules. The latter one is described as an interaction between permanent dipoles and between permanent and induced dipoles (Abdullah, 2009). Equation 5 illustrates the total interfacial energy consisted of the interfacial energy due to dispersive part “ E_d ” and the polar part, “ E_p ”;

$$E_{\text{total}} = E_d + E_p \quad (5)$$

In Fig. 6 the non-bonded energy value versus time step for three different atom pairs in the presence of the magnetic field of $B=0$ and 4 [T] is exhibited. As seen, in all cases, the absolute value of the non-bonded energy is increased by applying an external magnetic field.

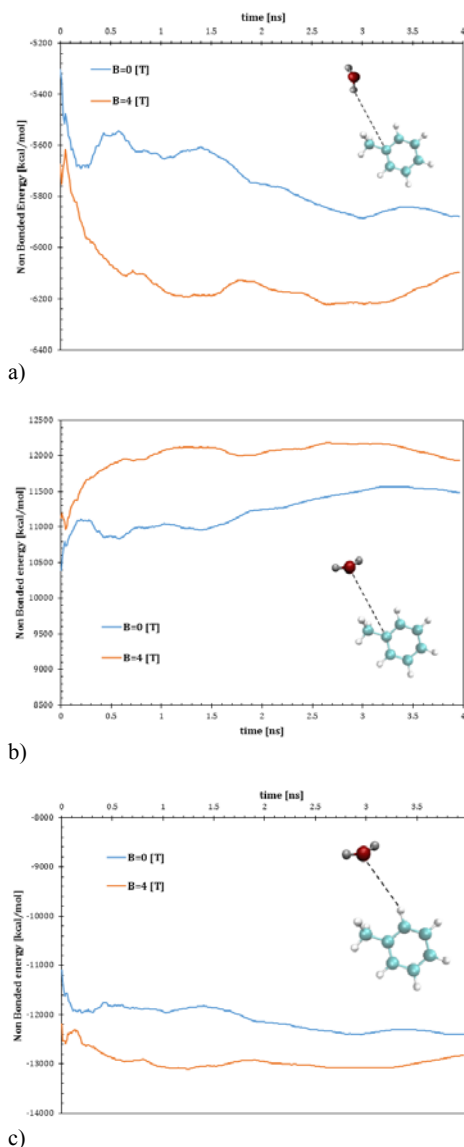


Fig. 6. The rolling average of the Non-bonded energy values versus time step for two types of atom pairs in the presence of $B=0$ and $B=4$ [T]; (a) Hydrogen in water and carbon in toluene, (b) Oxygen in water and carbon in toluene, (c) Oxygen in water and hydrogen in toluene

This increase in the amount of non-bonded energy causes an enhancement in two parts of interfacial energy. Consequently, the total value of the interfacial energy increases. Then, the potential level for interaction is getting more (as seen in Fig. 4), and IFT value is decreased. It is interesting to

mention that, in the presence of the magnetic field (i.e., $B=4$ [T]), the Lorentz force is strong enough to overcome the repulsive force between toluene and water molecules.

4. CONCLUSION

In the present study, the effect of an external magnetic field on the toluene-water interface was examined. The RDF and integration RDF plots showed that the tendency for the interaction between two types of molecules is changed in the presence of an external magnetic field. The potential for interaction is decreased at $B=2$ [T] and is increased at $B=4$, and more. Through the MD simulation of the toluene-water system, the changes in IFT value have been observed. This modification in structural behavior of interface system is attributed to the effect of applying magnetic field. The results indicate that applying a rather strong magnetic field can decrease the IFT values. In fact, the intense magnetic field shows the emulsifying behavior for the toluene-water system. The preparation of emulsions requires energy to disperse the organic phase in water, and applying magnetic field provides this energy. It means that, applying magnetic field (enough strong magnetic field) by increasing the interfacial energy, reduces the IFT. The reduction in the water-toluene IFT, stabilizes the water-in-toluene emulsion.

Since, using chemical additive to the system, is not environmentally friendly and sometimes is costly, we should mention that the magnetic treatment sound useful technique in emulsification.

ACKNOWLEDGEMENTS

The authors wish to express their gratitude to Prof. Yoshiro Masuda, and Dr. Yunfeng Liang from The University of Tokyo, Japan, for their assistance.

REFERENCES

- Abdullah S. (2009). *Molecular Simulation Study Of Diverting Materials Used In Matrix Acidizing*. Texas AandM University.
- Alejandre, J., D. J. Tildesley and G. A. Chapela (1995). Molecular dynamics simulation of the orthobaric densities and surface tension of water. *The Journal of Chemical Physics* 102(11), 4574–4583.
- Alkali, S. O. F., I. Of and A. S. P. Fluidstheir (2011). *Alkaline-Surfactant Flooding*.
- Allen, M. (2004). Introduction to molecular dynamics simulation. *Computational Soft Matter: From Synthetic Polymers to Proteins, Lecture Notes*, 23(2), 1–28.
- Alomair, O., S. Alqabandi, M. Malallah and A. Alajmi (2015). Experimental investigation of crude oil emulsion physicochemical properties and demulsifier dosage prediction.

- Society of Petroleum Engineers - SPE/IATMI Asia Pacific Oil and Gas Conference and Exhibition, APOGCE 2015*, 1–24.
- Brooks, B. R., C. L. Brooks III, A. D. M. J. (2010). NIH Public Access. *The Journal of Computational Chemistry* 124(2), 11–28.
- Carrillo Beber, V., L. Taveira Caleiro, K. Rossi de Aguiar, J. O. Joswig, U. Pereira Rodrigues Filho, P. L. M. Noeske, K. Rischka and W. L. Cavalcanti (2015). Molecular simulation on carbon dioxide fixation routes towards synthesis of precursors for innovative urethanes. *Applied Adhesion Science* 3(1).
- Chang, K.-T. and C. I. Weng (2006). The effect of an external magnetic field on the structure of liquid water using molecular dynamics simulation. *Journal of Applied Physics* 100(4), 043917.
- Chen, X., L. Hou, W. Li, S. Li and Y. Chen (2018). Molecular dynamics simulation of magnetic field influence on waxy crude oil. *Journal of Molecular Liquids* 249, 1052–1059.
- Donahue, D. J., F. E. Bartell, F. E. Bartell, U. Michigan and A. Arbor (1961). *The boundary tension at water-organic liquid interfaces*. 56(1), 480–484.
- Giorgino, T. (2014). Computing 1-D atomic densities in macromolecular simulations: The density profile tool for VMD. *Computer Physics Communications* 185(1), 317–322.
- Giorgino, T. (2019). Computing diffusion coefficients in macromolecular simulations: the Diffusion Coefficient Tool for VMD. *Journal of Open Source Software* 4(41), 1698.
- Guo, B., H. B. Han and F. Chai (2011). Influence of magnetic field on microstructural and dynamic properties of sodium, magnesium and calcium ions. *Transactions of Nonferrous Metals Society of China (English Edition)*, 21(SUPPL. 2).
- Han, H. (2013). *Mechanism Studies of Magnetic Effect on Transport Behavior in Reverse Osmosis Seawater Desalination*. Harbin Institute of Technology.
- Hanwell, M. D., D. E. Curtis, D. C. Lonie, T. Vandermeersch, E. Zurek and G. R. Hutchison (2012). Avogadro: An advanced semantic chemical editor, visualization, and analysis platform. *Journal of Cheminformatics* 4(8), 17.
- Huang, X., J. Sun, K. Lv, J. Liu and H. Shen (2018). An alternative method to enhance w/o emulsion stability using modified dimer acid and its application in oil based drilling fluids. *RSC Advances* 8(46), 26318–26324.
- Humphrey, W., A. Dalke and K. Schulten (1996). *VMD: Visual Molecular Dynamics*. 7855 (December 1995), 33–38.
- Israelachvili, J. (2011). *Intermolecular and Surface Forces*, 2nd ed.; Academic Press: London, 1992.
- Iwasaka, M. and S. Ueno (1998). Structure of water molecules under 14 T magnetic field. *Journal of Applied Physics* 83(11), 6459–6461.
- Jennings, H. Y. (1967). *The Effect of Temperature and Pressure on the Interfacial Tension of Benzene-Water and Normal Decane-Water*. 329, 323–329.
- Jideani, Y. M. and V. A. (2018). We are IntechOpen, the world's leading publisher of Open Access books Built by scientists, for scientists TOP 1%. In *Science and Technology Behind Nanoemulsions* (pp. 65–81).
- Khajeh, K., H. Aminfar, Y. Masuda and M. Mohammadpourfard (2020). Implementation of magnetic field force in molecular dynamics algorithm: NAMD source code version 2.12. *Journal of Molecular Modeling* 26(5), 106.
- Kilpatrick, P. K. (2012). Water-in-crude oil emulsion stabilization: Review and unanswered questions. *Energy and Fuels* 26(7), 4017–4026.
- Kumar, S. and V. Mahto (2017). Emulsification of Indian heavy crude oil using a novel surfactant for pipeline transportation. *Petroleum Science* 14(2), 372–382.
- Kunieda, M., K. Nakaoka, Y. Liang, C. R. Miranda, A. Ueda, S. Takahashi, H. Okabe and T. Matsuoka (2010). Self-accumulation of aromatics at the oil-water interface through weak hydrogen bonding. *Journal of the American Chemical Society* 132(51), 18281–18286.
- Langevin, D., S. Poteau, I. Hénaut and J. F. Argillier (2004). Crude Oil Emulsion Properties and Their Application to Heavy Oil Transportation. *Oil and Gas Science and Technology* 59(5), 511–521.
- Martínez, L., R. Andrade, E. G. Birgin and J. M. Martínez (2009). *Software News and Update Packmol: A Package for Building Initial Configurations*.
- Mikami, Y., Y. Liang, T. Matsuoka and E. S. Boek (2013). Molecular dynamics simulations of asphaltene at the oil-water interface: From nanoaggregation to thin-film formation. *Energy and Fuels* 27(4), 1838–1845.
- Moosavi, F. and M. Gholizadeh (2014). Magnetic effects on the solvent properties investigated by molecular dynamics simulation. *Journal of Magnetism and Magnetic Materials* 354, 239–247.
- Moran, K., A. Yeung and J. Masliyah (1999). Measuring interfacial tensions of micrometer-sized droplets: A novel micromechanical technique. *Langmuir* 15(24), 8497–8504.
- Newman, G. H. and L. A. Habra (1971). *The Effect*

of Temperature and Pressure on the Interracial Tension of Water Against Methane-Normal Decane Mixtures.

- NIST. (2009). NIST Reference Fluid Thermodynamic and Transport Properties — REFPROP (student version). *Database*. Retrieved from <http://www.boulder.nist.gov/div838/theory/refprop/MINIREF/MINIREF.HTM>
- Numbers, R., T. Shapes and I. Netlogo (1998). *Programming Guide*. 1–22.
- Peng, J., Q. Liu, Z. Xu and J. Masliyah (2012). *Novel Magnetic Demulsifier for Water Removal from Diluted Bitumen Emulsion*.
- Phillips, J. C., R. Braun, W. E. I. Wang, J. Gumbart, E. Tajkhorshid, E. Villa, ... K. Schulten(2005). Scalable molecular dynamics with NAMD. *Journal of Computational Chemistry* 26(16), 1781–1802.
- Ruiz-Morales, Y. and O. C. Mullins (2015). Coarse-grained molecular simulations to investigate asphaltenes at the oil-water interface. *Energy and Fuels* 29(3), 1597–1609.
- Saeedi Dehaghani, A. M. and M. H. Badizad (2018). Effect of magnetic field treatment on interfacial tension of CTAB nano-emulsion: Developing a novel agent for enhanced oil recovery. *Journal of Molecular Liquids* 261, 107–114.
- Souleyman, A. Issaka (2015). Review on the Fundamental Aspects of Petroleum Oil Emulsions and Techniques of Demulsification. *Journal of Petroleum & Environmental Engineering* 6(2), 1000214.
- Spreiter, Q. and M. Walter (1999). Classical molecular dynamics simulation with the velocity verlet algorithm at strong external magnetic fields. *Journal of Computational Physics* 152(1), 102–119.
- Ta, A. P. and M. A. Wilsonb (1993). *Viewpoint 9 - Molecular structure of aqueous interfaces* 284, 271–298.
- Taylor, P., M. Andresen, P. Stenius and M. Andresen(2007). *Journal of Dispersion Science and Technology Water - in - oil Emulsions Stabilized by Hydrophobized Microfibrillated Cellulose Water-in-oil Emulsions Stabilized by Hydrophobized Microfibrillated Cellulose*. (July 2015).
- Taylor, P., Y. Sun, W. Wang, H. Chen, C. Li, Y. Sun, ... C. Li (2011). *Autoxidation of Unsaturated Lipids in Food Emulsion Autoxidation of Unsaturated Lipids in*. (October 2013), 37–41.
- Tung, N. P., Vuong, N. Van, B. Quang, K. Long, N. Q. Vinh, and P. Viet (2001). *SPE 68749 Studying the Mechanism of Magnetic Field Influence on Paraffin Crude Oil Viscosity and Wax Deposition Reductions*.
- Wong, S. F., J. S. Lim and S. S. Dol (2015). *Journal of Petroleum Science and Engineering Crude oil emulsion: A review on formation, classification and stability of water-in-oil emulsions*. 135, 498–504.
- Yang, W. M., H. An, S. K. Chou, S. Vedharaji, R. Vallinagam, M. Balaji, ... K. J. E. Chua (2013). *Emulsion fuel with novel nano-organic additives for diesel engine application* 104(x), 726–731.